



SPECIAL ISSUE: 2026 Emerging Investigator Issue

Ultrasonic vibration enabled cold manufacturing of high thermal conductive Cu/Diamond composites

Boyang Wu^{1,2,3}, Bangliang Cao^{1,2,3}, Xiangyang Yu^{1,2,3}, Yu Zhang^{1,2,3,4*}, Zixian Zhao^{1,2,3}, Wenzhe Bao^{1,2,3}, Jianhuan Shao^{1,2,3}, Degui Yu^{1,2,3}, Jie Dong^{1,2,3}, Xiaodi Liu^{1,2,3} and Jiang Ma^{1,2,3*}

ABSTRACT The development of electronic components has put forward higher requirements for heat dissipation materials, manifested in the pursuit of higher thermal conductivity and lower thermal expansion. Cu/Diamond composite, combining excellent thermal conductive performance and process ability. However, it is limited by strict preparation conditions, such as high temperature and pressure, or complex intermediate medium coating. This work proposes a one-step and heat-source-free cold manufacturing method to fabricate Cu/Diamond composite under room temperature and a low pressure of ~16 MPa within seconds via ultrasonic vibration. The applied pressure decreased by 200 to 500 times, and the required temperature was only 20% of the commonly used high-temperature and high-pressure sintering (HTHP) method. Direct metallurgical bonding between the interfaces of Cu particles and solid embedding of diamond in the Cu matrix was achieved, leading to the high yield strength of the composite (150 MPa). Following the proposed strategy, a maximum diamond proportion of about 60% in the composite can be prepared, which shows high thermal conductivity over 1043 W/(m K) and a minor thermal expansion coefficient less than 10 (10^{-6} K^{-1}). In addition, composites of different complex shapes were readily fabricated through the flexible method. The heat dissipation application test reveals its better thermal management performance than commercial Al_2O_3 and AlN. Our results demonstrate that ultrasonic vibration assisted cold manufacturing is a facile and efficient way to prepare Cu/Diamond composite with excellent properties. Loose preparation conditions empower it with industrial production potential.

Keywords: ultrasonic vibrations, Cu/Diamond composite, thermal conductivity, thermal expansion coefficient

INTRODUCTION

The development of electronic components follows the famous Moore's law [1], exponentially increasing the quantity of heat-generating electronic devices, proposing higher requirements for heat dissipation [2,3]. Thermal management materials, a crucial part of the cooling system to release the heat generated during

the operation of the system and effectively dissipate the heat from electronic devices to the external environment, require a higher thermal conductivity [4,5]. Crystalline silicon is the main universal material to fabricate electronic components with a thermal conductivity of only 150 W/(m K) [6]. The accumulated heat may cause damage to the circuit board, so materials with higher thermal conductivity are necessary to encapsulate to guide the heat away.

Diamond is the substance with the highest thermal conductivity in nature, which can reach 1200–2500 W/(m K) [7–11]. However, it cannot be directly used for heat dissipation in electronic devices. One reason is its high hardness and brittleness [12], which make it difficult to machine into devices [13,14]. The other is its high cost, which is unacceptable in commercial production [15]. Metal/diamond composites are widely applied in the thermal management of high-power electronic devices due to their high thermal conductivity and low coefficient of thermal expansion (CTE). In the selection of matrix materials, it is essential to balance high thermal conductivity with a matched CTE. Compare to common high-thermal-conductivity metals such as Ag and Al, Cu has the closest CTE to that of diamond. This significantly reduces thermal mismatch-induced interfacial stress, enhancing the composite's reliability and service life under thermal cycling. Therefore, incorporating diamond particles into a Cu matrix represents a highly promising strategy [16]. In addition, Cu itself features low cost, mature fabrication processes, and high thermal conductivity of approximately 400 W/(m K), which further consolidates its dominant position in the Metal/Diamond composite [17,18]. Cu/Diamond composite will take advantage of the machinability of Cu and maintain the high thermal conductivity of diamond. HTHP is one of the main existing fabrication methods of the Cu/Diamond composite [19–21]. Yoshida *et al.* [22] prepared a Cu/Diamond composite with a maximum thermal conductivity of 742 W/(m K) using the HTHP method under a temperature of approximately 1473 K and pressure over 4.5 GPa. Another practical method is sparking plasma sintering (SPS) [23–25]. Ren *et al.* [26] prepared a Cu/Diamond composite with a maximum thermal conductivity of 657 W/(m K) using SPS under the temperature of approximately 1213 K and pressure of 40 MPa. The other is vacuum hot press

¹ State Key Laboratory of Radio Frequency Heterogeneous Integration, Shenzhen University, Shenzhen 518060, China

² Shenzhen Key Laboratory of High Performance Nontraditional Manufacturing, Shenzhen University, Shenzhen 518060, China

³ Guangdong Provincial Key Laboratory of Micro/Nano Optomechanics Engineering, Shenzhen University, Shenzhen 518060, China

⁴ School of Materials Science and Engineering, Wuhan University of Technology, Wuhan 430070, China

* Corresponding author (email: 1910293023@email.szu.edu.cn; majiang@szu.edu.cn)

sintering (VHPS) [27,28], which requires a strict high-temperature and pressure preparation environment.

The poor wettability between Cu and diamond makes chemical reactions difficult to occur, which promotes the formation of defects at the Cu/Diamond interface and weakens the interfacial bonding between them. The low-quality connection often results in a relatively low thermal conductivity, so enhancing the connectivity between Cu and diamond matrix is a key issue [29–31]. There are two methods to improve the connectivity between Cu and diamond. One is diamond surface metallization, such as magnetron sputtering (MS) [32], salt bath coating (SBC) [33], and so on. These methods coat the surface of diamond particles with a substance that exhibits good wettability with both Cu and diamond. Molina-Jordá *et al.* [33] fabricated a composite by depositing a 160 nm-thick titanium carbide (TiC) film on the diamond surface using the SBC method. Another method is adding active alloying elements to the Cu matrix [34], including alloy smelting (AS) [35], gas atomization (GA) [36], and so on. These methods involve doping Cu with a small quantity of active elements such as Ti, Zr, and Cr to improve the wettability of the Cu/Diamond interface. Li *et al.* [37] prepared Cu/Diamond composites with a Zr interlayer using the AS method. However, the materials added by these methods not only lower the overall thermal conductivity but also raise higher requirements for preparation conditions. There is an urgent need for a facile method that can fabricate Cu/Diamond composites at normal temperature and pressure without an intermediate medium, which is beneficial for reducing processing costs and raising production efficiency.

In this work, by adopting a new technology termed ultrasonic vibration cold manufacturing, the Cu/Diamond composites were successfully fabricated in a one-step molding under the environment of conventional room temperature and low pressure [38,39]. Direct metallurgical bonding occurs between Cu particle interfaces. The interface between Cu and diamond particles exhibits a 6–7 nm element diffusion zone, indicating that solid embedding between diamond and Cu matrix was achieved. The computed tomography (CT) and scanning electron microscope (SEM) results reveal that diamonds are evenly distributed, and no pores or cracks are present in the larger volume bulk sample. The high-quality bonding makes its high compression yield strength over 150 MPa. The maximum diamond volume proportion of the composite reaches up to 60%, the relatively high diamond proportion makes the maximum thermal conductivity of the composite over 1043 W/(m K), and the minor thermal expansion coefficient is less than 10 (10^{-6} K^{-1}). Meanwhile, it enables forming complex structures in one step, such as pentagrams and perforated squares. Compared to commercial heat sink materials, Al_2O_3 and AlN, the composite significantly improved heat dissipation for electronic components. Our results indicate that ultrasonic vibration assisted cold manufacturing enables one-step forming of Cu/Diamond composites under room temperature and low pressure without an intermediate medium. This efficient cold manufacturing method and the excellent heat dissipation performance of the product endow it with potential industrial production applications.

EXPERIMENTAL SECTION

Cu and diamond powder sample preparation

The used Cu and diamond powders both exhibit purities

exceeding 99.99 (wt.%). The Cu powders, with an average particle size of 25.378 μm , were synthesized via an electrolytic process. The Ila type diamond powder, featuring a finer particle size distribution centered around 3.53 μm , was prepared by airflow fragmentation. All powders were sourced as commercial products. After accurately weighing the powders according to the experimental design, the powders were then homogenized using a planetary ball mixer (M201, Panasonic, Japan) for further ultrasonic vibration assisted forming.

UV cold manufacturing setup

The ultrasonic vibration (UV) equipment employed in this research comprises a transducer, a booster, a horn, and a control unit to adjust process parameters. The alternating current electrical signal initially converted into a 20 kHz vibration signal by the transducer made of piezoelectric material, then amplified to a peak amplitude of 40 μm via a booster, the amplified vibrations transmit to the sample by a horn (more details see Fig. 1a). During the UV process, the horn driven by pneumatic pressure of 400 kPa and contact with the Cu/Diamond powders directly. The ultrasonic vibration was triggered at the applied load of 300 N, then the horn worked at a frequency of 20 kHz and an amplitude of 100% ($\sim 40 \mu\text{m}$). The volume of diamond ranges from 0%–60%, corresponding to the input energies ranging from 500 to 2000 J. Even under the maximum energy condition of 2000 J, the processing time is less than 3 s due to the efficient and rapid energy dissipation. Different-shaped molds are used to process Cu/Diamond powder and fabricate samples with the corresponding shapes. A column matching the mold's shape is placed on top of the powder, and ultrasonic vibration is then applied to process this column. During this process, energy is transferred into the powder, enabling the one-step formation of Cu/Diamond samples in various shapes.

Monitoring of applied stress and temperature during UV cold manufacturing

An infrared imaging camera (Model 280d, Fotric, China) with a precision of 0.1 K was employed to monitor real-time temperature fluctuations during Cu/Diamond composite preparation; the image acquisition frequency was set as 12 Hz. To accurately measure the temperature inside the mold during the UV process, a thermocouple was put inside the powder to measure the temperature at a frequency of 100 Hz. A dynamometer (QLMH-P, QILI, China) was used to record the real-time force during the UV process. The mold was securely coupled to the force transducer via threaded mounting holes to ensure reliable force transmission. Force data were acquired using a high-speed data-acquisition card (National Instruments NI-9237), operating at a sampling frequency of 1000 Hz, and subsequently transmitted to a computer via a compact data acquisition chassis (cDAQ-9174, NI, USA).

Structural characterization of Cu/Diamond composite

An X-ray diffractometer (XRD, Miniflex 600, Rigaku, Japan) was utilized to investigate the phase composition of Cu and diamond before and after the UV process. The measurements were conducted using Cu K α radiation ($\lambda = 0.154 \text{ nm}$) over a 2θ angle range of 20° – 90° , with a scanning rate of 3° per minute and a scan interval of 0.02° . The scanned samples included the individual powders of Cu and diamond, as well as the processed surfaces of Cu/Diamond samples. An SEM (Quanta FEG 450,

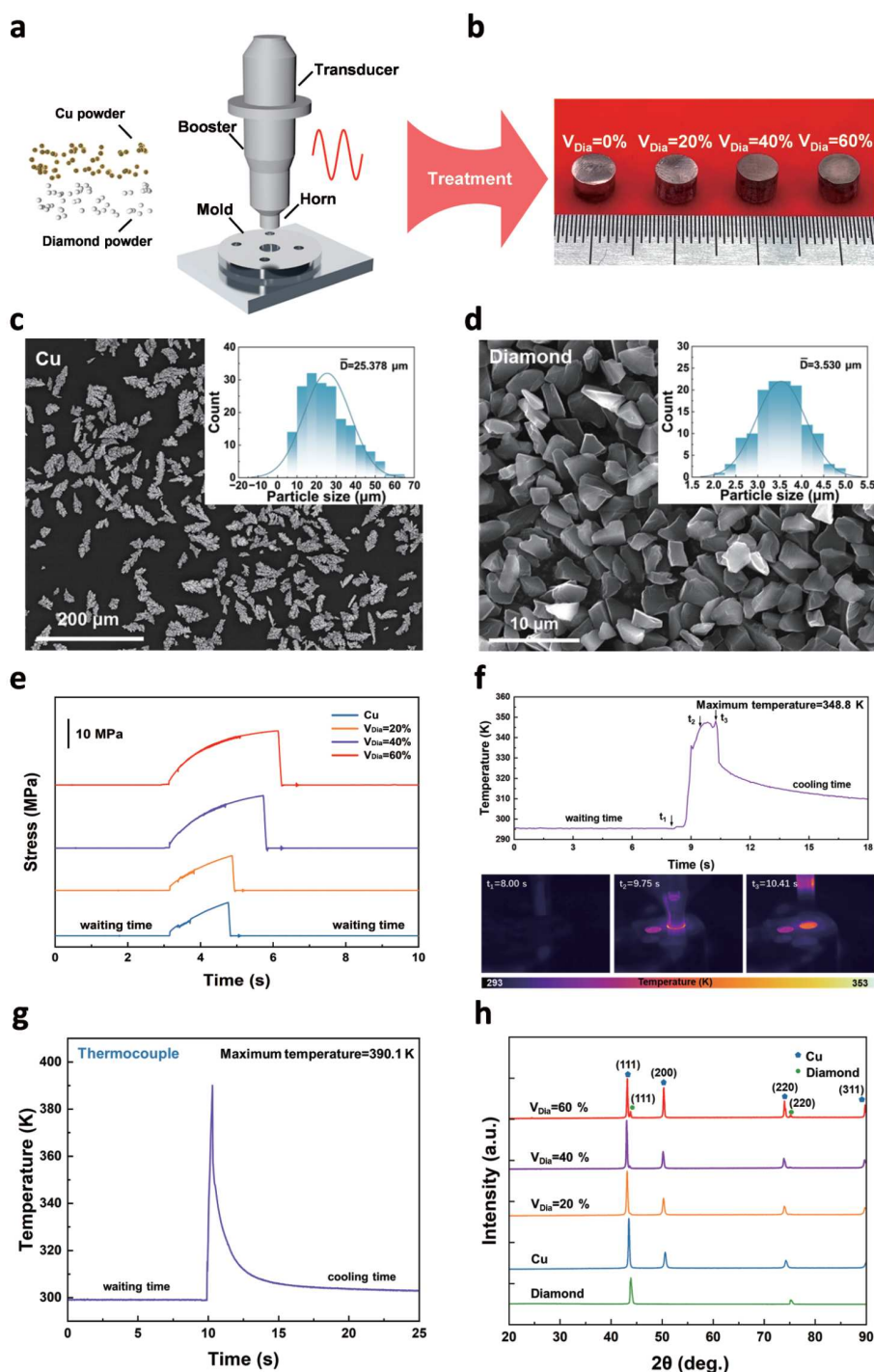


Figure 1 (a) Schematic illustration of ultrasonic vibration assisted forming and UV setup; (b) The photo of the composites with diamond volume proportions set at 0%, 20%, 40%, and 60%; (c) SEM morphology of the Cu powder, with an inset showing the statistical chart of their particle size; (d) SEM morphology of the diamond powder, with an inset showing the statistical chart of its particle size; (e) Applied stress during UV treatment of four samples with diamond volume proportions of 0%, 20%, 40%, and 60%; (f) The surface temperature curve and captured thermal infrared images during fabrication of the sample with a diamond volume proportion of 60%; (g) The temperature variation inside the sample with a diamond volume proportion of 60% during the ultrasonic vibration process was measured by a thermocouple; (h) XRD patterns of samples with diamond volume proportions of 0%, 20%, 40%, and 60%, as well as those of Cu and diamond powders.

FEI, USA) was employed to examine the morphology of Cu/Diamond composites at high magnification. A thin film with dimensions of 8 μm in length and 2 μm in width was prepared from the interface of Cu and diamond using the FEI Scios SEM/FIB dual-beam system for TEM test. The field emission trans-

mission electron microscope (TEM; Talos F200X G2, Thermo Fisher, USA) was used to analyze the TEM sample at the atomic scale. It was operated in bright-field mode, and the analysis encompassed selected-area electron diffraction (SAED) patterns, energy dispersive spectroscopy (EDS), and high-resolution

imaging. The internal defects of the Cu/Diamond composite material were characterized using a CT system (AX2000, ALWAYS IMAGING, China). The resolution is 1 μm , with a scanning step size of 2 μm .

Compression and hardness testing of Cu/Diamond composite

The compression tests were conducted on a mechanical testing machine (UMT-5105, SanSi, China) under room temperature with a strain rate of $\sim 1.9 \times 10^{-3} \text{ s}^{-1}$. The hardness of the Cu/Diamond composites was measured by a Vickers microhardness tester (FM-ARS9000, FUTURE-TECH, Japan) with a static load of 200 g, a holding time of 10 s, and at least 10 measurements per sample. The density of Cu/Diamond composites was measured by the Archimedes drainage method, with calculations based on the mass measured in water using an electronic analytical balance (FA224, LICHEN, China). Each sample was measured at least 10 times to obtain the mean data and variance.

Heat dissipation performance test with commercial products

The thermal and electrical conductivities of the Cu/Diamond composites were measured by a Hall effect tester (HMS-5500, Ecopia, Republic of Korea), and the coefficient of thermal expansion was measured by a thermal constant analyzer (TPS 2500S, HOT DISK, Sweden) within the temperature range from 300 to 400 K. The composites, along with alumina (Al_2O_3) and aluminum nitride (AlN) heat sinks, were fabricated into a cuboid with dimensions of $12 \times 20 \times 1 \text{ mm}^3$ and encapsulated on a custom-made circuit board. Thermal conductive adhesive was used to secure the thermal management materials to heat sinks of uniform specifications. Power was supplied using a programmable AC power source (IT7321, ITECH, America). The system comprised four operational zones, operating at a power of 30 W. Real-time temperature measurements were concurrently conducted using a multi-channel temperature tester (DC8016, DUCC, China) at a sampling frequency of 10 Hz, temperature change monitoring using an infrared imaging camera, boasting a precision of 0.1 K (Model 280d, Fotric, China) during operation.

RESULTS AND DISCUSSION

Cold manufacturing of Cu/Diamond composites

The whole procedure of ultrasonic vibration assisted forming of Cu/Diamond composites is shown in Fig. 1a. At the beginning, the uniformly mixed Cu and diamond powders were put into the die hole of the mold, a circular die hole with a diameter of 5 mm, and a completely coordinated horn was used in this experiment. Then the horn slowly descends under the drive of air pressure and contact with powders to release continuous ultrasonic vibrations for 3 s. After that, the mixed Cu/Diamond powders were quickly bonded into a bulk one. The photo of the bonded sample is shown in Fig. 1b, it displays the cylindrical samples with a diameter of 5 mm, and the volume proportions of diamond increased from left to right as 0%, 20%, 40%, and 60%. In this Cu/Diamond composite, Cu serves as the matrix material, achieving bonding with diamond particles through its remarkable plastic deformation capability. This property originates from the softness and high atomic mobility during the processing of Cu [35], which facilitates interfacial bonding between the particles. Despite the inherent difficulty in directly bonding diamond particles, results demonstrate they still form dense bulk

composites without cracks or defects, even when the diamond volume proportion reaches up to 60%. When attempting to fabricate a Cu/Diamond composite with diamond volume proportions of 70% and 80%, a complete bulk sample could not be prepared because the reduced Cu matrix is insufficient to effectively cover and immobilize each diamond particle. Fig. 1c shows the morphology of Cu particles used in this experiment, which do not show a regular shape like spherical or cubic, but they look like “leaves” with an average particle size of 25.378 μm . This irregular shape results in a larger contact surface area between powders, which is beneficial for forming [40]. Fig. 1d shows diamond particles with a particle size of 3.5 μm . It can be observed that the fractured diamond material exhibits irregular shapes and possesses a large surface area. It has unstable crystal faces, which facilitate easier bonding with the Cu matrix.

Fig. 1e shows the applied stress during the fabrication of the composite with different diamond volume proportions. The curve consists of two parts: waiting time and processing time. During the waiting time, the stress remains unchanged without fluctuations, and increases when the horn contacts the mixed powder and begins to vibrate. Although the applied stress is positively correlated with the increase of the diamond volume proportion, the maximum stress to fabricate a 60% diamond proportion composite is only 16 MPa, which is 200–500 times lower than other methods for preparing Cu/Diamond composites [19–21]. Additionally, the temperature variation during the process is also a critical process parameter. To ensure measurement accuracy, this study employed two independent temperature monitoring methods, which were the infrared thermometer and the thermocouple. Fig. 1f presents the average temperature profile and thermal images detected by the infrared thermometer. The results consist of three specific times, t_1 , t_2 , and t_3 , corresponding to the moments of the horn just contacting powders, during the process, and the horn going to leave the sample after the process, respectively. The temperature rises intensely, with a maximum temperature reaching 348.8 K during the vibration process. Furthermore, Fig. 1g presents the temperature variation curve measured by a highly sensitive thermocouple, which indicates a peak temperature of 390.1 K. Although it is 40 K higher than the thermal profile captured by the infrared imaging camera, the thermocouple’s measurement results are more convincing because it directly contacted the mixed powder during testing. Overall, the temperature rise during the composites fabrication process is only about 120 K. The maximum temperature is 390.1 K, which is much less than the recrystallization temperature of both Cu and diamond, also less than the temperature at which Cu starts to oxidize in air (453 K) [41]. What’s more, the required temperature is only 20% of the commonly used HTHP approach [19–21]. The effect of this instantaneous temperature rise can be ignored, so the composite can be considered fabricated under room temperature.

Structural characterization of the composite

Fig. 1h is the X-ray patterns of Cu powder and diamond powder, and processed composites with different diamond proportions. The diamond powder reveals a single phase; it has two main peaks in 2θ of 43.9° and 75.3° corresponding to the (111) and (220) crystal planes, which match well with PDF#75-0219. The Cu powders also reveal a single phase, it has three main peaks in 2θ of 43.3° , 50.4° , and 74.13° corresponding to the (111), (200),

and (220) crystal planes, which match well with PDF#04-0836. These results confirmed the high-purity Cu powder and diamond powder raw materials. After being processed into the composite, with the increasing proportion of diamond, the intensity of the diffraction diamond peaks increases, and samples formed a composite with simple mechanical mixing. Because apart from the original Cu and diamond peaks, there is no new peak that appears after the UV process. This simple mechanical mixing can also be observed by back-scattered electron micrographs, in Fig. 2a–c, the composite consists of two phases, the black regions correspond to diamond particles, whereas the gray areas denote the Cu matrix. The diamond particles are uniformly distributed within the Cu matrix, and the particle size is similar to the original one, indicating that the diamond particles exhibit good homogeneity and will not fracture by ultrasonic vibrations. No diamonds have detached from the Cu metal matrix in the composites, and the diamond particles are closely bonded with the Cu matrix; no pores or cracks

were observed, showing reliable bonding quality.

The bonding quality of Cu/Diamond composites was further characterized by high-resolution CT. Fig. 2d, e depict the axial relative density distributions of cylindrical samples with diamond volume proportions of 30% and 60%, respectively. The diagrammatic sketch of the scan direction is shown in the inset beside Fig. 2d, e. In the density distribution maps, the green regions represent the Cu matrix due to their higher density than diamond, while the orange-yellow regions correspond to diamond particles. In the sample with a 30% diamond volume proportion, as shown in Fig. 2d, diamond particles exhibit a uniform distribution. When the diamond volume proportion increases to 60%, the particles undergo further homogeneous dispersion, causing the matrix color to transition from green to yellow. This indicates that diamond achieves a uniform distribution within the Cu matrix. Concurrently, experimental observations reveal a gradual decrease in sample density with increasing diamond content. Despite the decrease in density, no

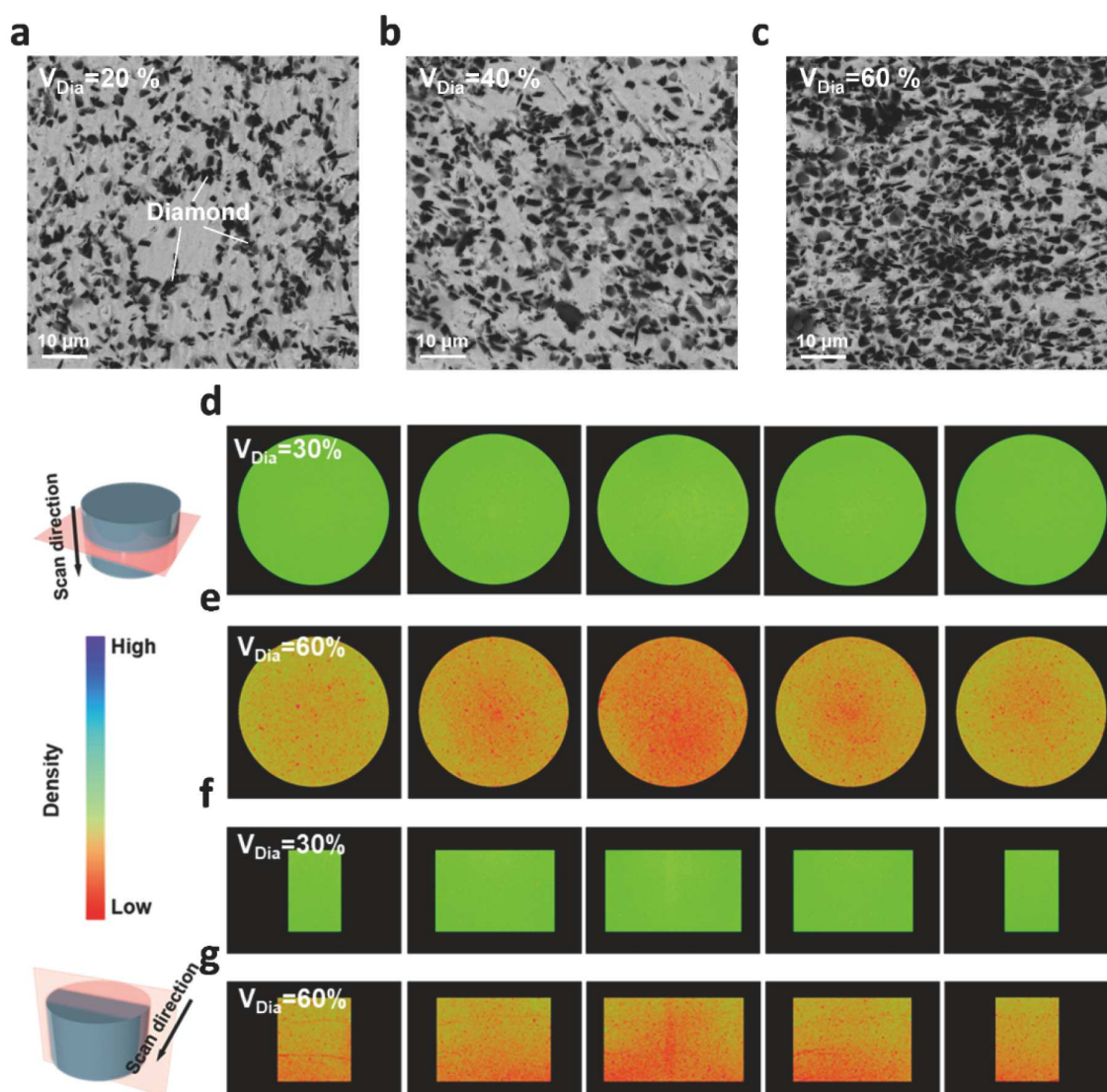


Figure 2 Back-scattered electron micrographs morphology image of the Cu/Diamond composite with a diamond volume proportion of (a) 20%, (b) 40%, (c) 60%; CT relative density distribution map obtained from axial scanning of a Cu/Diamond composite with a diamond volume proportion of (d) 30% and (e) 60%, CT relative density distribution map obtained from radial scanning of a Cu/Diamond composite with a diamond volume proportion of (f) 30% and (g) 60%.

discernible defects were observed in the microstructure. In some regions of the sample in Fig. 2e, there exists an area with even lower density, which is attributed to the agglomeration of diamond particles. This phenomenon is associated with the powder mixing time: as the diamond content increases, the Cu matrix becomes less able to permeate and flow due to the reduced interparticle spacing of diamond particles. This issue can be improved by increasing both the mixing time and mixing speed when the diamond volume proportion rises. Fig. 2f, g show the relative density distributions of cylindrical samples scanned radially with diamond volume proportions of 30% and 60%. The diagrammatic sketch of the scan direction is shown in the inset beside Fig. 2f, g; the scanned results are similar to axial scanning. Based on three-dimensional high-resolution CT scan results, the well-bonding quality of Cu/Diamond composite can be confirmed.

The interface of the composite is a core component of the composite, which will significantly impact both mechanical and thermal conductive properties [42]. It has been discussed in Fig. 2 that the particle size of diamond is kept the same after UV, and the Cu particles are bonded together to form the matrix of the composite. High-resolution TEM was conducted on both the interface of Cu particles and the interface of Cu and diamond particles. Fig. 3a displays the interface of two Cu particles, although a distinct interface can be seen between them, no visible holes or cracks appear on the interface, indicating that the two particles were bonded well with each other. It should be mentioned that the distinct interface shown in Fig. 3a does not appear on all Cu particles; it is an intermediate state before it is well bonded, and it can be imagined that most of the interface will disappear when inputting higher ultrasonic vibration energy. By analyzing the mapping in Fig. 3b and the line scan profile of Cu,

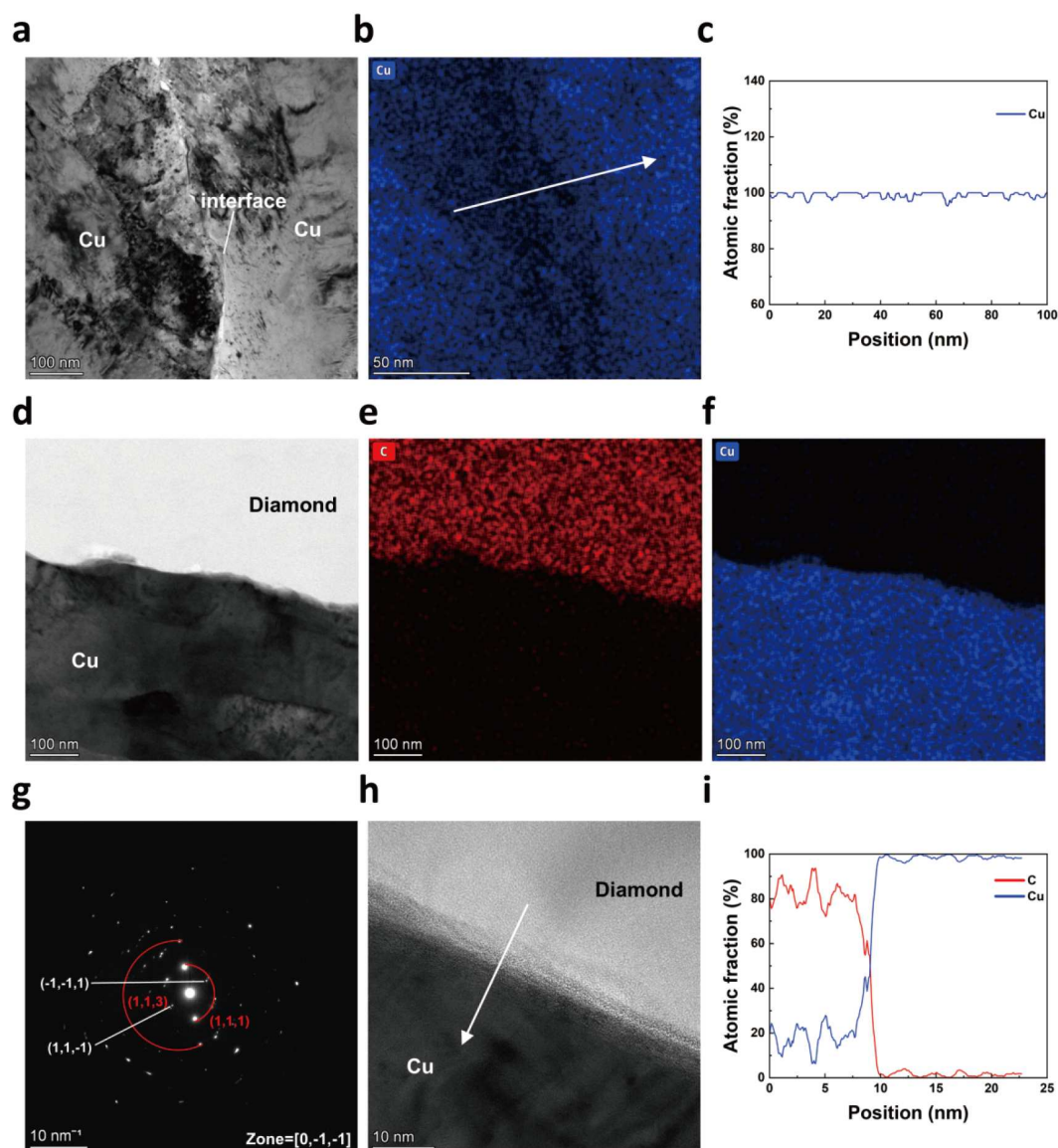


Figure 3 (a) TEM image of the bonding interface between Cu particles; (b) EDS map of the interface of two Cu particles; (c) The line scan profile of Cu element along the white arrow in (b); (d) TEM image of the interface between Cu and diamond particles; (e) EDS map of C element; (f) EDS map of Cu element; (g) Selected area electron diffraction (SEAD) taken from the region of (d), the interface of Cu and diamond; (h) HR-TEM images of the interface of Cu and diamond particles; (i) The line scan profile of C and Cu elements along the white arrow in (h).

it is confirmed that Cu content is kept similar across the interface without fluctuations, which implies that even the Cu particles at the interface can also be treated as a single unit. The UV imparts high energy to the edge of particles and atoms at the particle boundaries, which absorb this energy and diffuse toward defects at the interfaces. Meanwhile, the particles undergo rapid mutual friction under ultrasonic vibration, generating heat that accelerates atomic diffusion rates. Softer Cu particles undergo plastic deformation to fill defects at the interfaces. Ultimately, diffusion layers of C atoms and Cu atoms form at the interfaces, creating a reliable metallurgical bond at low temperatures [43,44].

The TEM morphology shows interface of Cu and diamond is demonstrated in Fig. 3d, the Cu and diamond particle bonded together with each other directly without any intermediate medium, and the amplified morphology of the interface shows in Fig. 3h, it reveals high-quality direct bonding of Cu and diamond without cracks and pores at the atomic scale, width about of 6–7 nm element expansion can be seen cooperate with the line scan across the interface in Fig. 3i. which means that Cu and diamond have mixed each other in the interface and solid embedding of diamond in the Cu matrix was achieved [45]. From the EDS maps in Fig. 3e, f, they show that the upper half region is diamond and the lower part is Cu. The color of each map displays no changes near the interface, implying there is no intermediate medium between Cu and diamond. To further confirm the direct bonding of Cu and diamond, Fig. 3g reveals the SEAD of the Cu/Diamond interface in Fig. 3d, which consisted of two sets of spots, one of which is the red diffraction ring from polycrystalline Cu, the rings consisted of the nano-sized Cu grain with different orientations of which is matching (111) and (113) crystal planes. However, the diamond phase shows some scattered spots, which indicates that the grain size is much bigger than Cu [46], and the spot matches with the (111) crystal plane of diamond, further confirming the formation of the composite. Overall, the TEM results portend the high-quality direct bonding of both Cu and Cu particles and Cu and diamond particles.

Mechanical and thermophysical properties characterization

Fig. 4a illustrates the densities of Cu/Diamond composites with diamond volume proportions of 0%, 20%, 40%, and 60%. The sample with 60% diamond volume proportion exhibits the lowest density (5.67 g/cm^3). A linear decrease in density is observed with increasing diamond content, which is consistent with CT measurements in Fig. 2, because diamond has a lower density than Cu, so that the composite with a higher diamond proportion shows lower density. Fig. 4b shows the evolution of Vickers hardness of the composites within the range of 0% to 40% diamond volume proportion. Hardness increases gradually because the Cu matrix acts as the main deformation-bearing phase under deformation, resulting in a slight increase in hardness from 30.02 HV to 68.24 HV. When the diamond proportion reaches 60%, the harder diamond phase becomes the dominant phase, leading to a sharp rise in hardness to 206.4 HV [47]. Furthermore, the compression stress-strain curve of the Cu/Diamond composite is depicted in Fig. 4c, four samples yield at the strength of 150 MPa, and the 20% diamond volume proportion sample shows the best plasticity of 35%. However, the difference lies in the work hardening ability of samples, the engineering strain of pure Cu increased sharply to 450 MPa

when deformed to higher strain, which portends the best work hardening ability. While with the increasing diamond proportion, the work hardening ability decreased, manifested in a slight increase of strength when deformed to higher strain, and even the 60% diamond volume proportion sample fractured at a strain of 12.9% due to the brittleness of the diamond proportion. Ultrasonic vibration enhances the flowability and compaction of the material, defects between particles are filled with the severe plastic deformation of Cu particles, but the shape of diamond will not change so much, and its show much higher compressive strength and higher hardness than Cu. The high compressive strength comes from the hindrance of diamond to the dislocations of Cu, because it can not cross diamond and continue to transmit, which all significantly improves the overall densification of the composite material and provides the basis for its high compressive strength.

Fig. 4d shows the electrical conductivity of samples with diamond volume proportions of 0% to 60%. Due to the low electrical conductivity of diamond [48], the electrical conductivity of the samples decreases linearly with increasing diamond volume fraction. When the diamond volume proportion reached 60%, the composite exhibited the lowest electrical conductivity of $2.25 \times 10^4 \text{ S/cm}$, approaching the regime of insulating materials [49]. Fig. 4e displays the curves of the thermal expansion coefficient of composites within the temperature range of 300 to 400 K. The coefficient of thermal expansion increases at 300 K and then decreases, and maintains a level with gentle fluctuations between 330 to 400 K. The higher volume proportion of diamond corresponds to a lower thermal expansion coefficient, and the average thermal expansion coefficient of the composite with 60% diamond volume proportion is lower than $10 \times 10^{-6} \text{ K}^{-1}$. The relatively low thermal expansion coefficient is crucial to increasing the thermal stability in the field of electronic packaging. The thermal conductivity of composites with diamond volume proportions of 0% to 60% is shown in Fig. 4f, as the volume proportions of diamond increase, the thermal conductivity rises continuously, reaching 1043 W/(m K) for the sample with a 60% diamond volume proportion, this is a relatively high value compared to other approaches. That's because Cu conducts heat by interaction and collision between electrons, while diamond transfers heat via lattice vibrations, involving the absorption and emission of phonons. To estimate the thermal conductivity of a Cu/Diamond composite using the Maxwell-Eucken Model, it can be calculated by the following formula [34]:

$$\lambda_c = \lambda_m \frac{2(1 - V_d)\lambda_m + (1 + 2V_d)\lambda_d}{(2 + V_d)\lambda_m + (1 - V_d)\lambda_d},$$

where λ_c is the thermal conductivity of Cu/Diamond composites; λ_m is the thermal conductivity of Cu matrix; λ_d is the thermal conductivity of the diamond reinforcing particles; and V_d is the volume proportion of diamond spherical particles in the Cu/Diamond composites. By substituting the values of λ_m as 400 W/(m K) and λ_d as 2200 W/(m K) into the model, the calculated thermal conductivity when the V_d is 60% is approximately 1075 W/(m K) . The experimental thermal conductivity achieved 97.02% of the theoretical value, significantly surpassing results obtained via other methods for fabricating Cu/Diamond composites. The excellent performance benefits from exceptionally high heat transfer efficiency and strong interfacial bonding at the Cu-diamond atomic diffusion layer. At a dia-

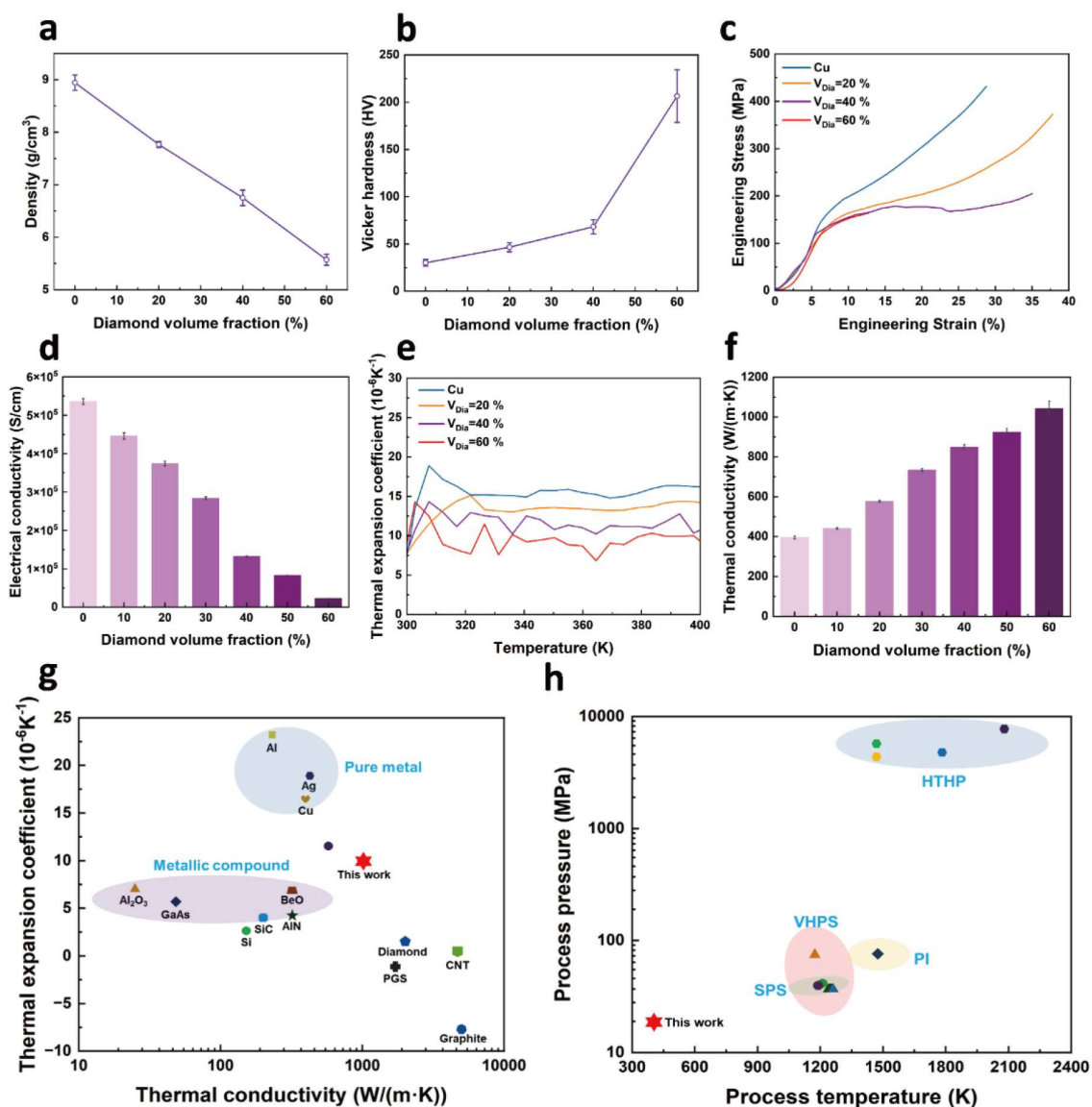


Figure 4 (a) Densities of Cu/Diamond composites, (b) Vickers hardness diagram of Cu/Diamond composites, (c) compression engineering strain-stress curves of Cu/Diamond composites, (d) electrical conductivity of Cu/Diamond composites, (e) thermal expansion coefficients of Cu/Diamond composites, and (f) thermal conductivity of Cu/Diamond composites with diamond volume proportions of 0%, 20%, 40%, and 60%; (g) Statistical chart of thermal conductivity and thermal expansion coefficient for commonly used thermal conductive materials; (h) Statistical chart of temperature and pressure parameters for commonly used fabrication techniques of Cu/Diamond composites.

mond volume proportion of 20%, the high Cu content gives the composite with a good combination of strength and ductility, enabling facile machining and forming; it is thus suitable for structural-thermal integrated components such as equipment heat dissipation enclosures and brackets. For the sample with 40% diamond volume proportion, the thermal conductivity reaches 850 W/(m K), which can meet the heat dissipation requirements of most electronic packaging and high-power devices such as AI/GPU chips and lasers. When the diamond volume proportion is increased to 60%, the thermal conductivity of the composite is further enhanced, with a concomitant increase in brittleness, making it applicable to fields with extreme thermal dissipation demands but relatively relaxed mechanical property requirements, such as aerospace airborne equipment and laser weapon heat dissipation systems.

The high thermal conductivity and low coefficient of thermal expansion of the Cu/Diamond composite make it an ideal option among thermal management materials. Fig. 4g presents a statistical comparison of the thermal conductivity and coefficient of thermal expansion of commonly used thermal conductive materials. It demonstrates that the Cu/Diamond composite shows more outstanding performance than pure metal materials as well as metal compound materials. Though the pure diamond, pyrolytic graphite sheet (PGS), graphene and carbon nanotube (CNT) possess higher thermal conductivity and lower coefficient of thermal expansion than the Cu/Diamond composite, diamonds are difficult to machining into products due to their high hardness and brittleness; and pyrolytic PGS, graphene and CNT limited by the anisotropic nature of thermal conductivity properties manifested in the superior thermal conductivity of

graphite sheet, graphene, and carbon nanotubes only available in their in-plane while other plane is 2–3 orders of magnitude lower than it [43–45], so Cu/Diamond composite is the most ideal option as a new generation of thermal management materials with high thermal conductivity and low coefficient of thermal expansion.

Fig. 4h shows a comparison between our UV cold manufacture and other fabrication methods for Cu/Diamond composites. The current methods for processing Cu/Diamond composites include HTHP, SPS, VHPS, and PI. The HTHP approach needs to be carried out at approximately 1500 to 2000 K and under a pressure of 4 to 8 GPa [19,22,50,51]. Both the SPS and VHPS methods involve preparation temperatures close to 1200 K and pressures ranging from 40 to 80 MPa [26,52–54]. For the PI method, the preparation pressure and temperature are approximately 80 MPa and 1500 K [55], respectively. In contrast, our UV cold manufacturing method operates at a maximum temperature of 390.1 K and a maximum applied pressure of 16 MPa. This low-temperature and low-pressure approach reduces energy consumption during the processing. Additionally, it shortens the processing time from the previous 20 min to just a few seconds, thereby enhancing processing efficiency.

Showcase of formed composite with complex shape

In addition to the excellent mechanical and thermal management properties of the Cu/Diamond composite, it also possesses

highly flexible one-step forming ability. Fig. 5 shows samples with various shapes formed by UV with a metallic luster characteristic of Cu. Fig. 5a is a hexagon component, Fig. 5b is a square sample with a round hole, this designed shape enables easy assembly and disassembly during practical use. Fig. 5c is a triangle sample, Fig. 5d is a pentagon, and Fig. 5e is a square. All these samples were fabricated in seconds under UV with a high replication rate. The SEM back-scattered electrons images in Fig. 5a–c show that the corners of the sample are of good quality at the microscopic level, the sample's sharp corners remained intact without fractures or cracks when subjected to angles ranging from 60° to 120°. This high forming quality is attributed to the effective powder flow and complete filling of the mold cavity during the UV cold manufacture. While using other methods to produce the structure in Fig. 5, post-processing like wire electrical discharge machining or laser cutting is necessary. These methods are time-consuming and inevitably generate high temperatures, forming Cu oxide and reducing the sample's thermal conductivity.

Encapsulated circuit board test

The one-step formed composite can be directly encapsulated on the circuit board to evaluate the heat dissipation performance of Cu/Diamond composites. As illustrated in Fig. 6a, two commonly used thermal management materials, AlN and Al₂O₃, along with our Cu/Diamond composites, were simultaneously placed on electronic components within the circuit board for

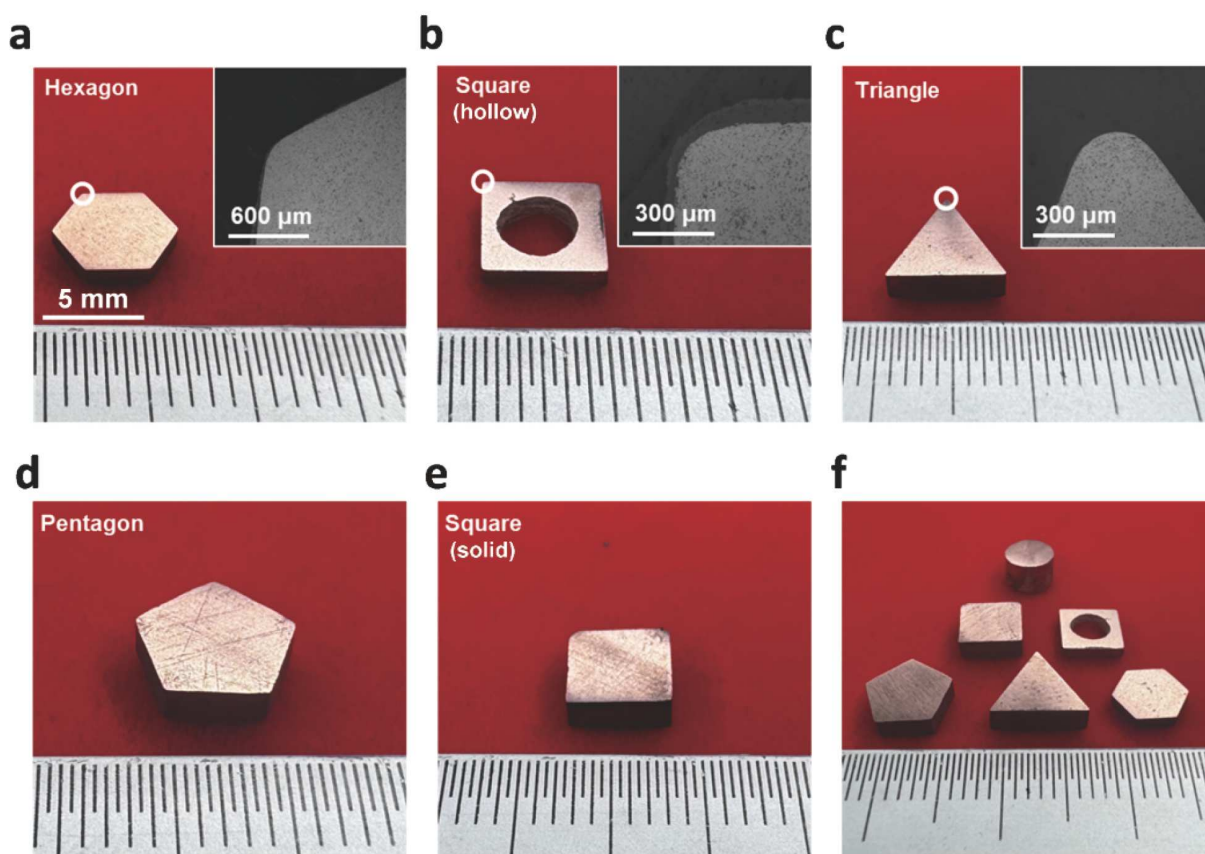


Figure 5 Photos of (a) a hexagon Cu/Diamond composite, (b) a square with a circular hole at its center of Cu/Diamond composite, and (c) a triangle Cu/Diamond composite, with insets of SEM images showing the corner regions of the samples; (d) Photos of a pentagon Cu/Diamond composite; (e) Photos of a square Cu/Diamond composite; (f) The photo of all the complex parts fabricated by ultrasonic vibration, one-step forming.

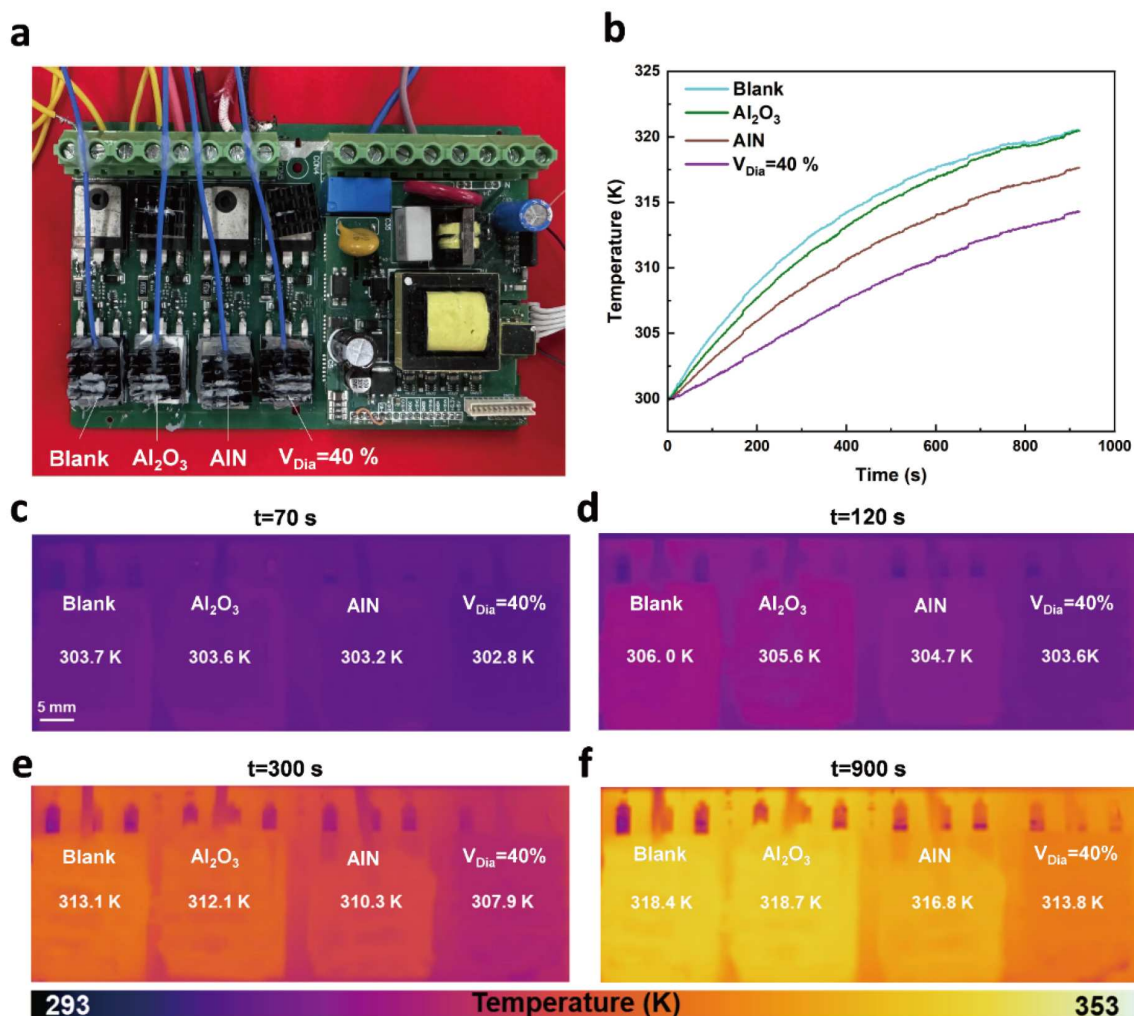


Figure 6 (a) Photo of the sample with a 40% volume proportion of diamond, along with Al₂O₃ and AlN, encapsulated within a circuit board; (b) Temperature variations during the continuous operation of the circuit board for a duration of 915 s; Thermal infrared images of the circuit boards at (c) 70 s, (d) 120 s, (e) 300 s, and (f) 900 s of operation.

comparative testing. To balance the thermal conductivity and mechanical properties of these composites and evaluate their average heat dissipation capacity, the sample with a diamond volume proportion of 40% was selected for the tests. Meanwhile, a component without any thermal management material is used for comparison. During the test, the temperature variation to evaluate the heat dissipation capacity was recorded and is shown in Fig. 6b. The rate of temperature rise gradually decreases as the heat generation power of the circuit board gradually reaches equilibrium with its heat dissipation power. The maximum temperature in the region without any heat sink materials reached approximately 320 K, while in the area using our Cu/Diamond composite, the maximum temperature was around 314 K, the maximum temperatures decreased by approximately 6 and 3 K when compared with commonly used Al₂O₃ and AlN heat sinks. Fig. 6c–f displays infrared thermal images of the heat sink surface captured at different moments when the power supply is operating; our Cu/Diamond composite also performs well at each moment. In practical applications, the operating power of electronic components often exceeds 30 W. High thermal conductivity Cu/Diamond composites will further reduce component temperatures when operating in higher

power, and their heat dissipation capacity improves with increasing diamond content, exhibiting excellent effectiveness in practical applications.

Mechanism of cold manufacturing and high thermal conductivity

As shown in the Fig. 7, at the beginning, Cu and diamond powders are mixed together randomly, these particles are not smooth sphere so the edge of powders have numerous defects, like indicated by Fig. 7a. When the ultrasonic vibrations begins as shown in Fig. 7b, the energy generated by high-frequency vibrations can be absorbed by atoms in the material, especially in the areas with a large number of defects at the edge of particles. This high frequency vibrations provide additional energy support for atomic diffusion [56], significantly increasing the probability of atoms (especially carbon atoms with strong bonding in diamond) detaching from the lattice and migrating [57]. Driven by the coupling of vibrations and force, the softer Cu particle undergoes plastic deformation to fill the gaps between particles, and the more and deeper defects bite into each other. As the vibration continues, as shown in Fig. 7c, some heat is generated due to vibration induced by mechanical friction and further increases the atomic migration rate, so mutual

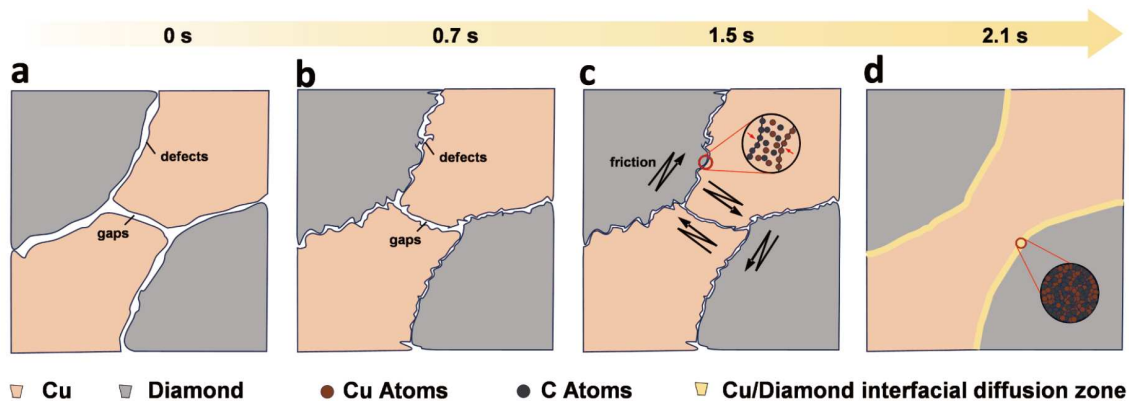


Figure 7 (a) Schematic diagram of the initial state of Cu and diamond powders showing some initial defects and gaps before ultrasonic vibration start; (b) Schematic diagram of state showing more defects in the edge of particle and less gaps after 0.8 s of UV; (c) Schematic diagram of Cu and C atoms diffusion after 1.5 s of ultrasonic vibration, with an inset showing the migration direction of atoms in the gaps; (d) Schematic diagram of bulk composite formed by UV, with an inset showing the atomic-scale illustration of interfacial diffusion zone between Cu and diamond.

diffusion occurs between Cu and C atoms, like the inset of Fig. 7c, and higher level severe plastic deformation of Cu particles fills the remaining cracks. Cu particles connected with each other to form the matrix of composites, and the mutual diffusion of Cu and C atoms was frozen to form reliable diffusion bonding. All particles become a bulk one in the end, as shown in Fig. 7d.

UV enables direct metallurgical bonding between Cu and diamond which significantly enhances the thermal conductivity of the composite, primarily due to the unique physico-chemical effects it induces at the interface: the vibration energy promotes atomic diffusion and rearrangement of Cu and diamond at the interface to form the mutual diffusion layer, it has favorable phonon-matching characteristics and acts as an ideal “phonon bridge” rather than a complete barrier, effectively mitigating the large vibrational mismatch between Cu (electron-mediated heat transfer) and diamond (phonon-mediated heat transfer), thus significantly reducing interfacial thermal resistance [58]. Additionally, the UV enhances material flowability and compaction, markedly increasing the overall densification of the composite, reducing phonon-scattering defects such as pores and micro-cracks, and establishing more efficient pathways for heat transfer [59].

CONCLUSIONS

In summary, a one-step and heat-source-free cold manufacturing method for fabricating Cu/Diamond composites through UV under room temperature and low-pressure conditions has been proposed. Microscopic observation and CT analysis revealed that the formed composites show no visible pores or cracks, and the diamonds were uniformly distributed within the Cu matrix. TEM analysis results indicate that direct metallurgical bonding has been achieved between Cu particles. Meanwhile, an atomic diffusion zone with a thickness of 6–7 nm was discovered at the interface between Cu and diamond particles, implying that diamond particles have formed a solid embedding structure with Cu matrix, which effectively addresses the issue of poor wettability between Cu and diamond. Additionally, the high-quality bonding enables it to achieve a high compressive yield strength exceeding 150 MPa. The maximum proportion of diamond in the composite is 60%, with a thermal conductivity

exceeding 1043 W/(m K) and a coefficient of thermal expansion less than $10 \times 10^{-6} \text{ K}^{-1}$, demonstrating excellent thermal properties. Additionally, it allows for the one-step molding of various complex structures, which has potential for large-scale industrial production. Compared to currently commonly used heat sink materials such as Al_2O_3 and AlN, packaging tests in circuit boards have demonstrated their superior heat dissipation of electronic components. The excellent properties and loose preparation conditions make UV-cold-manufactured Cu/Diamond composites a candidate for commercial thermal management materials.

Received 29 November 2025; accepted 3 February 2026;
published online 25 February 2026

- Shalf J. The future of computing beyond Moore’s Law. *Phil Trans R Soc A*, 2020, 378: 20190061
- Bahiraei M, Heshmatian S. Electronics cooling with nanofluids: a critical review. *Energy Convers Manage*, 2018, 172: 438–456
- Hagio T, Park JH, Naruse Y, *et al.* Electrodeposition of nano-diamond/copper composite platings: improved interfacial adhesion between diamond and copper via formation of silicon carbide on diamond surface. *Surf Coatings Tech*, 2020, 403: 126322
- Park J, Kim D, Kim H, *et al.* Thermal radiative copper oxide layer for enhancing heat dissipation of metal surface. *Nanomaterials*, 2021, 11: 2819
- Zhang L, Li Y, Li S, *et al.* Fabrication of titanium and copper-coated diamond/copper composites via selective laser melting. *Micromachines*, 2022, 13: 724
- Moore AL, Shi L. Emerging challenges and materials for thermal management of electronics. *Mater Today*, 2014, 17: 163–174
- Kidalov SV, Shakhov FM. Thermal conductivity of diamond composites. *Materials*, 2009, 2: 2467–2495
- Liang X, Jia C, Chu K, *et al.* Thermal conductivity and microstructure of Al/diamond composites with Ti-coated diamond particles consolidated by spark plasma sintering. *J Composite Mater*, 2011, 46: 1127–1136
- Ma S, Zhao N, Shi C, *et al.* Mo_2C coating on diamond: different effects on thermal conductivity of diamond/Al and Diamond/Cu composites. *Appl Surf Sci*, 2017, 402: 372–383
- Wu J, Zhang H, Zhang Y, *et al.* Effect of copper content on the thermal conductivity and thermal expansion of Al-Cu/Diamond composites. *Mater Des*, 2012, 39: 87–92
- Xue C, Yu JK, Zhu XM. Thermal properties of diamond/SiC/Al com-

- posites with high volume fractions. *Mater Des*, 2011, 32: 4225–4229
- 12 Xu B, Tian Y. Superhard materials: recent research progress and prospects. *Sci China Mater*, 2015, 58: 132–142
- 13 Bu YQ, Wang P, Nie AM, *et al.* Room-temperature plasticity in diamond. *Sci China Technol Sci*, 2020, 64: 32–36
- 14 Nie A, Zhao Z, Xu B, *et al.* Microstructure engineering in diamond-based materials. *Nat Mater*, 2025, 24: 1172–1185
- 15 Yu G, Dutta JM, Jones CR, Potentials of SiC as a gyrotron window material. In Proceedings of the Joint 29th International Conference on Infrared and Millimeter Waves/12th International Conference on Terahertz Electronics, Univ Karlsruhe, Karlsruhe, Germany, 2004, pp. 299–300
- 16 Arai S, Ueda M. Fabrication of high thermal conductivity Cu/Diamond composites at ambient temperature and pressure. *AIP Adv*, 2019, 9: 085309
- 17 Nunes D, Correia JB, Carvalho PA, *et al.* Production of Cu/Diamond composites for first-wall heat sinks. *Fusion Eng Des*, 2011, 86: 2589–2592
- 18 Wei TR, Qin Y, Deng T, *et al.* Copper chalcogenide thermoelectric materials. *Sci China Mater*, 2019, 62: 8–24
- 19 Ekimov EA, Suetin NV, Popovich AF, *et al.* Thermal conductivity of diamond composites sintered under high pressures. *Diamond Relat Mater*, 2008, 17: 838–843
- 20 Guillemet T, Geffroy PM, Heintz JM, *et al.* An innovative process to fabricate copper/diamond composite films for thermal management applications. *Compos Part A-Appl Sci Manufacturing*, 2012, 43: 1746–1753
- 21 Zain-ul-abdein M, Raza K, Khalid FA, *et al.* Numerical investigation of the effect of interfacial thermal resistance upon the thermal conductivity of copper/diamond composites. *Mater Des*, 2015, 86: 248–258
- 22 Yoshida K, Morigami H. Thermal properties of diamond/copper composite material. *MicroElectron Reliability*, 2004, 44: 303–308
- 23 Chu K, Liu Z, Jia C, *et al.* Thermal conductivity of SPS consolidated Cu/Diamond composites with Cr-coated diamond particles. *J Alloys Compd*, 2010, 490: 453–458
- 24 Ukhina AV, Dudina DV, Esikov MA, *et al.* The influence of morphology and composition of metal-carbide coatings deposited on the diamond surface on the properties of copper-diamond composites. *Surf Coatings Tech*, 2020, 401: 126272
- 25 Zhang X, Xu M, Cao S, *et al.* Enhanced thermal conductivity of diamond/copper composite fabricated through doping with rare-earth oxide Sc_2O_3 . *Diamond Relat Mater*, 2020, 104: 107755
- 26 Ren S, Shen X, Guo C, *et al.* Effect of coating on the microstructure and thermal conductivities of Diamond-Cu composites prepared by powder metallurgy. *Compos Sci Tech*, 2011, 71: 1550–1555
- 27 Luo F, Jiang X, Sun H, *et al.* Microstructures, mechanical and thermal properties of diamonds and graphene hybrid reinforced laminated Cu matrix composites by vacuum hot pressing. *Vacuum*, 2023, 207: 111610
- 28 Zhang C, Cai Z, Tang Y, *et al.* Microstructure and thermal behavior of Diamond/Cu composites: effects of surface modification. *Diamond Relat Mater*, 2018, 86: 98–108
- 29 Ishida N, Kato K, Suzuki N, *et al.* Preparation of amino group functionalized diamond using photocatalyst and thermal conductivity of diamond/copper composite by electroplating. *Diamond Relat Mater*, 2021, 118: 108509
- 30 Raza K, Khalid FA. Optimization of sintering parameters for diamond-copper composites in conventional sintering and their thermal conductivity. *J Alloys Compd*, 2014, 615: 111–118
- 31 Schubert T, Trindade B, Weißgärber T, *et al.* Interfacial design of Cu-based composites prepared by powder metallurgy for heat sink applications. *Mater Sci Eng-A*, 2008, 475: 39–44
- 32 Bai H, Ma N, Lang J, *et al.* Effect of a new pretreatment on the microstructure and thermal conductivity of Cu/Diamond composites. *J Alloys Compd*, 2013, 580: 382–385
- 33 Molina-Jordá JM. Nano- and micro-/meso-scale engineered magnesium/diamond composites: novel materials for emerging challenges in thermal management. *Acta Mater*, 2015, 96: 101–110
- 34 Chen K, Leng X, Zhao R, *et al.* Progress in the copper-based diamond composites for thermal conductivity applications. *Crystals*, 2023, 13: 906
- 35 Weber L, Tavangar R. On the influence of active element content on the thermal conductivity and thermal expansion of Cu-X (X = Cr, B) diamond composites. *Scripta Mater*, 2007, 57: 988–991
- 36 Schubert T, Ciupiński Ł, Zieliński W, *et al.* Interfacial characterization of Cu/Diamond composites prepared by powder metallurgy for heat sink applications. *Scripta Mater*, 2008, 58: 263–266
- 37 Li J, Wang X, Qiao Y, *et al.* High thermal conductivity through interfacial layer optimization in diamond particles dispersed Zr-alloyed Cu matrix composites. *Scripta Mater*, 2015, 109: 72–75
- 38 Huang Z, Fu J, Li X, *et al.* Ultrasonic-assisted rapid cold welding of bulk metallic glasses. *Sci China Mater*, 2022, 65: 255–262
- 39 Yuan C, Lv Z, Pang C, *et al.* Ultrasonic-assisted plastic flow in a Zr-based metallic glass. *Sci China Mater*, 2021, 64: 448–459
- 40 Kozhar S, Dosta M, Antonyuk S, *et al.* DEM simulations of amorphous irregular shaped micrometer-sized titania agglomerates at compression. *Adv Powder Tech*, 2015, 26: 767–777
- 41 Fukumuro N, Adachi T, Yae S, *et al.* Influence of hydrogen on room temperature recrystallisation of electrodeposited Cu films: thermal desorption spectroscopy. *Trans IMF*, 2013, 89: 198–201
- 42 Mukhopadhyay S, Deopura BL, Alagiruswamy R. Interface behavior in polypropylene composites. *J ThermoPlast Composite Mater*, 2003, 16: 479–495
- 43 Li L, Li X, Huang Z, *et al.* Joining of metallic glasses in liquid via ultrasonic vibrations. *Nat Commun*, 2023, 14: 6305
- 44 Li ZL, Wang J, Yi SL, *et al.* Direct bonding of AZ31B and ZrO_2 induced by interfacial sono-oxidation reaction at a low temperature. *J Magnesium Alloys*, 2025, 13: 4316–4326
- 45 Meng B, Wang J, Chen M, *et al.* Study on the oxidation behavior of a novel thermal barrier coating system using the nanocrystalline coating as bonding coating on the single-crystal superalloy. *Corrosion Sci*, 2023, 225: 111591
- 46 Zhang Y, Zhao H, Yan YQ, *et al.* Ultrasonic-assisted fabrication of metallic glass composites. *J Non-Crystalline Solids*, 2022, 597: 121894
- 47 Hu W, Wen B, Huang Q, *et al.* Role of plastic deformation in tailoring ultrafine microstructure in nanotwinned diamond for enhanced hardness. *Sci China Mater*, 2017, 60: 178–185
- 48 Ullah M, Ahmed E, Hussain F, *et al.* Electrical conductivity enhancement by boron-doping in diamond using first principle calculations. *Appl Surf Sci*, 2015, 334: 40–44
- 49 Chen Q, Zhao Y, Li J, *et al.* Enhanced thermal constant B of diamond films for ultrahigh sensitivity negative temperature coefficient thermistors. *Sci China Mater*, 2024, 67: 3321–3329
- 50 Chen H, Jia C, Li S. Effect of sintering parameters on the microstructure and thermal conductivity of Diamond/Cu composites prepared by high pressure and high temperature infiltration. *Int J Miner Metall Mater*, 2013, 20: 180–186
- 51 He J, Wang X, Zhang Y, *et al.* Thermal conductivity of Cu-Zr/diamond composites produced by high temperature-high pressure method. *Compos Part B-Eng*, 2015, 68: 22–26
- 52 Chu K, Jia C, Guo H, *et al.* On the thermal conductivity of Cu-Zr/diamond composites. *Mater Des*, 2013, 45: 36–42
- 53 Zhang C, Wang R, Cai Z, *et al.* Effects of dual-layer coatings on microstructure and thermal conductivity of Diamond/Cu composites prepared by vacuum hot pressing. *Surf Coatings Tech*, 2015, 277: 299–307
- 54 Zhang Y, Zhang HL, Wu JH, *et al.* Enhanced thermal conductivity in copper matrix composites reinforced with titanium-coated diamond particles. *Scripta Mater*, 2011, 65: 1097–1100
- 55 Zhao C, Wang J. Enhanced mechanical properties in Diamond/Cu composites with chromium carbide coating for structural applications. *Mater Sci Eng-A*, 2013, 588: 221–227
- 56 Ma J, Yang C, Liu X, *et al.* Fast surface dynamics enabled cold joining of metallic glasses. *Sci Adv*, 2019, 5: eaax7256
- 57 Yang Z, Fujii Y, Lee FK, *et al.* Glass transition dynamics and surface layer mobility in unentangled polystyrene films. *Science*, 2010, 328: 1676–1679
- 58 Yang B, Tang Y, Xin Z, *et al.* Modulation of the interfacial thermal resistances of the w-AlN/Graphene/3C-SiC interface by nanoscale

nonplanar feature structures. *Appl Surf Sci*, 2024, 659: 159905
 59 Zhou Y, Ciarla R, Boonkird A, *et al.* Defects vibrations engineering for enhancing interfacial thermal transport in polymer composites. *Sci Adv*, 2025, 11: eadp6516

Acknowledgement The work was supported by the Science and Technology Innovation Commission of Shenzhen (RCJC20221008092730037 and 20220804091920001), the Key-Area Research and Development Program of Guangdong Province (2024B0101070001), and the Research Team Cultivation Program of Shenzhen University (2023QNT001). Liu X is supported by the National Natural Science Foundation of China (52201186). We thank the Instrumental Analysis Center of Shenzhen University for the assistance with the electron microscope.

Author contributions Wu B and Ma J conceived the project. Wu B performed the validation, investigation, data curation, and formal analysis, and wrote the original draft. Cao B, Yu X, Zhao Z, Bao W, Shao J, Dong J, and Liu X participated in the investigation. Dong J also contributed to data curation. Yu D was responsible for the software. Zhang Y and Ma J supervised the project, administered the project, provided resources and funding acquisition, and revised the manuscript. Zhang Y also participated in writing the original draft and conducting review & editing. Wu B and Ma J wrote and revised the paper.

Conflict of interest The authors declare that they have no conflict of interest.



Boyang Wu is currently a student at Shenzhen University. His research interest includes ultrasonic vibration-assisted manufacturing.



Yu Zhang received his MA degree from Shenzhen University in 2022. He is currently a PhD student at the School of Materials Science and Engineering, Wuhan University of Technology. His research interests include metallic glass, high-entropy alloys, and ultrasonic vibration-assisted manufacturing.



Jiang Ma received his BS degree in materials science and engineering from Southeast University in 2009 and his PhD degree from the Institute of Physics, Chinese Academy of Sciences (CAS), Beijing, in 2014. He is currently a professor at the College of Mechatronics and Control Engineering, Shenzhen University, and received the Outstanding Teacher Award of Shenzhen in 2018. His research interest includes the formation, functional application, and high-frequency dynamic loading behavior of metallic glasses.

超声波振动实现高热导率铜/金刚石复合材料的冷制造

吴搏扬^{1,2,3}, 曹帮亮^{1,2,3}, 喻向阳^{1,2,3}, 张宇^{1,2,3,4*}, 赵子贤^{1,2,3}, 包文哲^{1,2,3}, 邵坚桓^{1,2,3}, 余德贵^{1,2,3}, 董杰^{1,2,3}, 刘晓佛^{1,2,3}, 马将^{1,2,3*}

摘要 随着电子元件向高集成化、高性能化方向迅猛发展,对散热材料提出了更高的要求,表现为追求更高的热导率和更低的热膨胀系数.铜/金刚石复合材料这种结合了优异的导热性能和加工能力的材料需求激增,但其生产受到高温高压等严格的制备条件与复杂的中间介质镀膜的限制.在这项工作中,提出了一种一步成型、无热源的冷制造方法,在室温和16 MPa的低压下通过超声振动在几秒钟内制备了铜/金刚石复合材料.相比于常用的高温高压烧结(HTHP)方法,此方法压力降低200–500倍,温度仅为传统方法的20%.借助此技术,实现了铜颗粒界面之间的直接冶金结合和金刚石在铜基体中的固体嵌入,赋予复合材料150 MPa的高屈服强度.按照所提出的策略,可以制备金刚石比例最大约60%的复合材料,其热导率超过1043 W/(m K),热膨胀系数小于10 (10⁻⁶ K⁻¹).此外,通过该方法可以很容易制造出不同复杂形状的铜/金刚石复合材料.散热应用测试表明,其热管理性能优于商用的Al₂O₃和AlN材料.我们的结果表明,超声振动这种冷制造是制备铜/金刚石复合材料的一种简单有效的方法,同时使材料具有优异的性能,而宽松的制备条件使其具有工业生产潜力.